ISSN 1392–1320 MATERIALS SCIENCE (MEDŽIAGOTYRA). Vol. 13, No. 3. 2007

Formation of OVD Using Laser Interference Lithography

Tomas TAMULEVIČIUS[1,2*], Sigitas TAMULEVIČIUS[1,2], Mindaugas ANDRULEVIČIUS[2], Asta GUOBIENĖ[2,3], Linas PUODŽIUKYNAS[1,2], Giedrius JANUŠAS[3,4], Egidijus GRIŠKONIS[2,5]

[1]*Department of Physics, Kaunas University of Technology, Studentų 50, LT-51368 Kaunas, Lithuania*
[2]*Institute of Physical Electronics of Kaunas University of Technology, Savanorių 271, LT-50131, Kaunas, Lithuania*
[3]*International Studies Center, Kaunas University of Technology, Mickeviciaus 37, Kaunas, LT-44244, Lithuania*
[4]*Department of Applied Mathematics, Kaunas University of Technology, Studentų 50, LT-51368 Kaunas, Lithuania*
[5]*Department of General Chemistry, Kaunas University of Technology, Radvilėnų 19, LT-50254, Kaunas, Lithuania*

Received 07 August 2007; accepted 06 September 2007

In the present research we have fabricated and investigated optically variable devices (OVDs) (a system of submicron period surface relief diffraction gratings). For this purpose we have recorded interference pattern of two HeCd laser beams through a set of masks, forming contours of the image, in the photoresist (holographic technique). Changing the angles between the interfering beams we have achieved 0.7, 0.8, 0.9 and 1.2 μm period diffraction gratings. The microrelief of diffraction gratings from the resist was transferred to the metallic stamp using vacuum deposition (of Ag, Ni, Cu) and electrochemical nickel deposition. Diffraction efficiency of the diffraction gratings was measured experimentally and linear dimensions of diffraction gratings were defined by scanning electron microscopy (SEM) and atomic force microscopy (AFM). The main experimental results were compared with the computer simulations where the standard software ("PCGrate") was employed to calculate diffraction efficiency of the different depth of diffraction gratings for two wavelengths of the visible light. Influence of different sublayers used during the electrochemical deposition on the parameters (period, depth and shape) of the submicron structures was defined.

Keywords: optically variable devices (OVDs), laser interference lithography (LIL), submicron period diffraction gratings, diffraction efficiency.

1. INTRODUCTION

Recently, holograms and optically variable devices based on diffraction gratings have become widely used as anti-counterfeiting devices [1] where they are employed to protect banknotes, cheques and high security documents against [2] forgery. Diffractive optically variable image devices (DOVIDs or simply optically variable devices – OVDs) cannot be reproduced by conventional colour scanning or printing technique and therefore find a wide range of applications in document security field [3]. A basic feature of these devices has been the fine patterns of tracks designed to produce sharper definition of shapes and a greater brilliance of the image than with holograms under varying conditions of illumination [2, 4]. In the origination of these fine-scale patterns, the high lateral resolution and precise depth modulation is necessary were emerging lithography techniques enable formation of grating patterns with exact dimensions and spatial frequencies [2]. The resulting high resolution images can be accurately replicated as a nickel shim followed by mass production through embossing into thermoplastic polymers or hot stamping in metalized foil as the carrier for the iridescent image [1, 2, 5].

Emerging top-down lithography techniques like extreme ultraviolet lithography (EUV), nanoimprinting (NIL), electron beam lithography (EBL) and focused ion beam (FIB) patterning technologies are commonly used for nano and micro fabrication. However, they are encountering problems of either low speed, small patterning area or high cost equipment [6]. Maskless laser beam interference lithography (LIL) allows fast and large area periodical structures to be patterned with simple equipment. The LIL principle is based on the interference of two coherent lights to form a horizontal standing wave for grating pattern which can be recorded on the photoresist. The period of the grating is dependent on the wavelength of the used light and the half angle of two incident beams intersect [6]. Major element of the OVDs – 1D or 2D diffraction grating structures have been typically fabricated by LIL in the form of a dot matrix array. In these structures, the dot-shaped diffractive elements are comprised of gratings with a single frequency and orientation [5].

In resent articles [7, 8] we have presented surface relief transfer problems of micrometer range period diffraction gratings arising in technological steps from the master grating origination in the photoresit (LIL) [7] or silicon (contact optical photolithography) [8] to the thermoembossing in polymer replica (mass production). In this paper we describe technological steps and solutions of related technological problems of origination of the OVD stamp using LIL. The final product – original nickel shim includes submicron period diffraction gratings and micro text. Regularities of variation of features of submicrometer diffraction grating during the origination are discussed.

*Corresponding author. Tel.: +370-37-313432; fax.: +370-37-314423.
E-mail address: *t.tamulevicius@stud.ktu.lt* (T. Tamulevičius)

2. EXPERIMENTAL

2.1. OVD formation

For this experiment we have assembled an original lithographic stage with vacuum chuck and XYR alignment / positioning system (see Fig. 1). This system enables rotation of the mask holder as well as sample alignment / positioning system rotation by 15° degrees steps through 4 positions (clock wise) and 4 positions counter clock wise. These 9 angular positions, according to the direction of interference pattern orientation on the plane, are necessary for formation of various orientation diffraction gratings on the substrate. Superposition of the different expositions, using a set of mask, is performed with two translation stages including micrometer screws for X and Y alignment (travel range 20 mm); additionally several degrees in a rotational positioning can be performed using a screw. Interference pattern on the glass substrates covered (spincoated – 3000 rpm, 500 nm) with a Shipley MICROPOSIT® S1805® positive photoresist is formed using interference of two expanded and collimated HeCd laser beams (λ = 441.6 nm). Typical total exposition area is 20 mm by 20 mm. As a beam splitter, 556 nm period reflection diffraction grating is used. Laser beam collimating system is composed of micro objective, aperture and magnifying lens. The set of mirror pair positions (1-1', 2-2', 3-3') provides different interfering angles θ_1 , θ_2 , θ_3 (Fig. 1).

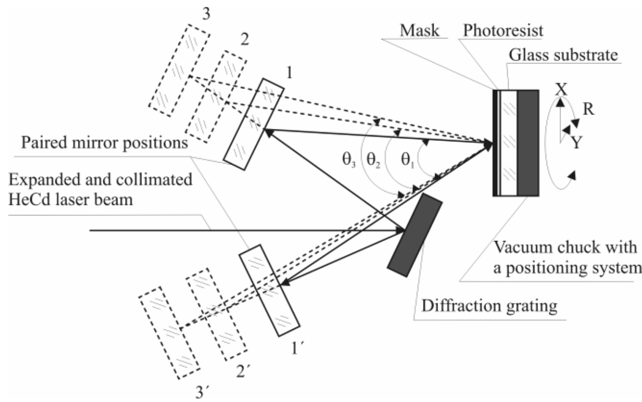

Fig. 1. Schematic LIL setup

Period of the interference pattern (d_i) in the photoresist depends on the laser wavelength and angle between the interfering beams [9]:

$$d_i = \frac{\lambda}{2\sin\frac{\theta_i}{2}} . \quad (1)$$

Where λ is a laser wavelength, θ_i is an angle between two interfering beams.

In our experiment the OVDs were formed using set of 8 masks for image contour formation, 3 different angles (31°, 34°, 37°, i. e. diffraction grating periods of 857 nm, 790 nm and 734 nm between the interfering HeCd laser beams) and 6 different sample orientations (0°, 15°, 30°, 45°, –30°, –15°) with respect to the interference pattern orientation. The masks also include micro text. After 8 expositions (time of each exposition 15 s) the photoresist was developed forming submicron relief of the OVD in the photoresist. Before electrochemical deposition the samples were covered using electron beam vacuum deposition by thin (100 nm) metallic layers and different sublayers (sample "A" – with copper, sample "B" – with nickel) were produced. The submicron relief was transferred to the nickel shim using electrochemical nickel deposition [7].

2.2. Analytical techniques

Optical properties and microrelief changes of diffraction gratings during different technological steps of manufacturing were measured with a diffraction stand. The main experimental results of optical evaluation were compared with the computer simulation results. Diffraction spectra (for –2°, –5°, –10°, –20°, –30°, –45° angle of incident light) were registered with the diffraction stand using HeNe (λ = 632.8 nm) and DPSS (λ = 532 nm) lasers and a photodiode. The following analytical methods were used to control microrelief in the nickel shim: optical microscope, atomic force microscope NANOTOP-206 (operating in a contact mode, cantilever force constant 0.3 N/m, lateral resolution 2 nm, vertical resolution 0.1 nm – 0.2 nm), ultra high resolution field emission scanning electron microscope Hitachi S-4800 (resolution 1.0 nm at 15 kV SE, electron beam voltage 0.1 kV – 30 kV).

3. RESULTS AND DISCUSSIONS

All measurements and simulations performed during different technological steps were done for two areas of the OVD that was composed of different period gratings: area named "R" consists of lower period (angle between the interfering beams θ = 31°) and area named "H" consist of higher period (θ = 34°).

3.1. Simulation of the diffraction efficiency of the sub micron period diffraction gratings

Using a standard software ("PCGrate") [10, 11] we have simulated the absolute diffraction efficiency of the sinusoidal profile diffraction grating in a photoresist, profile covered with thin metallic films (samples "A" and "B") and final profile transferred to the nickel shim. The simulations were performed following all the experimental details (including angles of incidence of laser beams, diffraction spectra spatial angular distribution). Two wavelengths of the visible light: λ = 532 nm and λ = 632.8 nm with a plane of polarization 45° with respect to the grooves of periodic structure were used in our calculations. Experimentally measuring angular distribution of the diffraction maxima, we have followed the changes of the period of diffraction gratings during the technological steps. One can see (Table 1) that the period of the diffraction grating increases after vacuum deposition of thin film (the structure expands) and it becomes the same like in photoresit after electrochemical deposition (the structure shrinks during electrodeposition). E. g. for the sample "A" the period in a "R" area after the development of the resist was 729 nm, after the vacuum deposition of copper it was increased to 745 nm and finally after the electrochemical deposition it has decreased to 724 nm (Table 1).

Table 1. Variations of the geometrical dimensions (obtained from the SEM, AFM measurements and simulation) of the diffraction grating after different technological steps: 1 – photoresist, 2 – photoresist coated with 100 nm Cu sublayer, 3 – metallic Ni stamp

Sample			Period, nm				Depth, nm
			Simulated	Expected	SEM	AFM	Simulated
1	A	R	729 ±12	790 (31°) ±24	–	–	95
		H	–	857 (34°) ±24	–	–	100
	B	R	–	790 (31°) ±24	–	–	100
		H	–	857 (34°) ±24	–	–	105
2	A (Cu)	R	745 ±12	790 (31°) ±24	–	–	85
		H	821 ±12	857 (34°) ±24	–	–	95
3	A (Cu)	R	724 ±12	790 (31°) ±24	728 ±5	714 ±5	75
		H	796 ±12	857 (34°) ±24	808 ±5	–	90
	B (Ni)	R	730 ±12	790 (31°) ±24	734 ±5	–	80
		H	800 ±12	857 (34°) ±24	800 ±5	778 ±5	85

These variations could be explained by the stress produced in the films during the technological steps.

In [12, 13] we have shown that comparing experimental and simulated values of the diffraction efficiency of the grating it is possible to determine geometry of the diffraction grating. Following the approach discussed in [12, 13] and comparing differences between the values of all (zeroth, first and second diffraction maxima) measured and simulated diffraction efficiencies we find values of the possible depth of the gratings in different technological steps. In Fig. 2 differences (named as "Difference, a.u.") between the measured and simulated values (average sum of squared differences between the simulated and experimentally measured diffraction efficiencies measured at different angles of incident light) of absolute diffraction efficiency (for 632.8 nm and 532 nm wavelengths) versus depth of the simulated diffraction grating are presented. Minima in the graph represent the expected depth of the grating.

3.2. SEM and AFM investigation

From the SEM and AFM measurements we have defined directly geometrical parameters of the diffraction gratings. The SEM micrographs of the final nickel shims (Fig. 3) are taken in a mixed backscattered and lower detector signal mode and the electron beam is perpendicular to the sample. In the micrographs one can see flat islands which correspond to the constructive interference (exposed area of the resist was removed during the development) and narrow channels which correspond to the destructive interference fringes. The fringe system is not uniform because of the additional interference from the mask, photoresist and glass substrate surfaces. The AFM measurements (Fig. 4) confirm depth and shape variation of the interference pattern registered with the SEM and measured of the diffraction efficiency. Simulation results and experimental results from the SEM and AFM measurements are presented in Table 1. One can see good correspondence between the experimental and simulated results. E. g. period of the diffraction grating of the sample "B", "H" area after the electrochemical deposition "3": period calculated according to the angle between interfering beams is 857 nm, calculated according to the diffraction angles – 797 nm, and defined with the SEM – 800 nm and finally measured with the AFM – 778 nm. From the simulation results one can see as well that the depth of the grating is decreasing during next technological steps, e. g. for the sample "A", "R" area of profile the depth of profile in photoresit "1" is 95 nm, after vacuum deposition "2" it is 85 nm and after electrochemical deposition "3" – 75 nm.

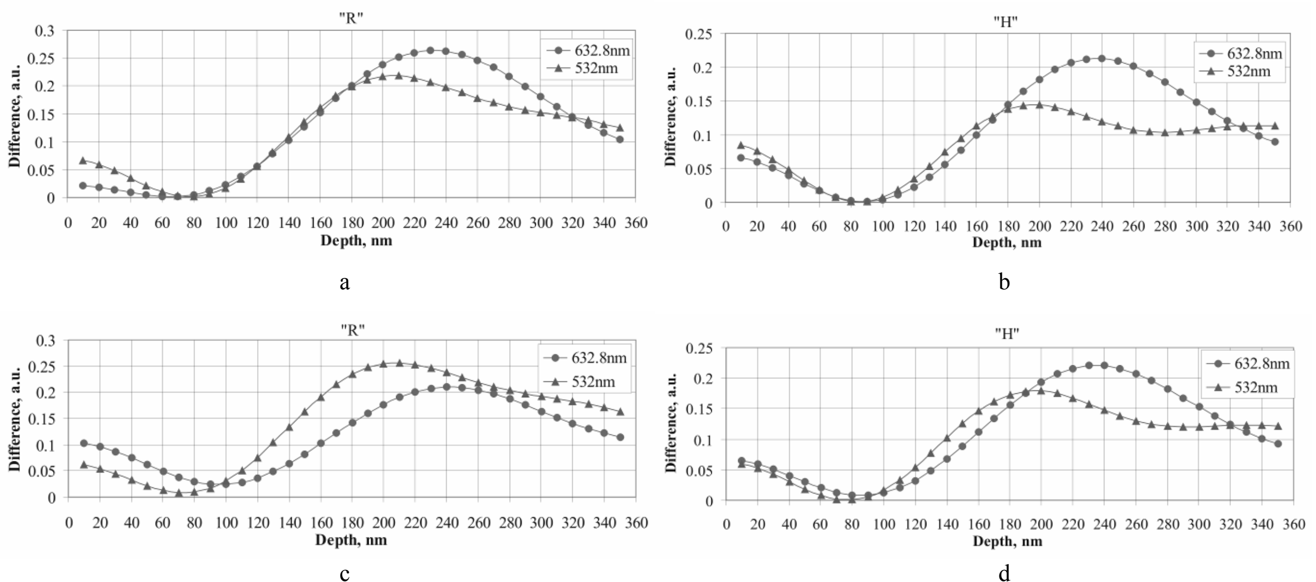

Fig. 2. Average sum of squared differences between the simulated and experimentally measured diffraction efficiencies (angles of incidence 0°, 5°, 10°, 15°, 20°, 25°) for two different wavelengths (633 nm, 532 nm): a – sample "3" "A" area "R", b – "3" "A" – "H", c – "3" "B" – "R", d – "3" "B" – "H"

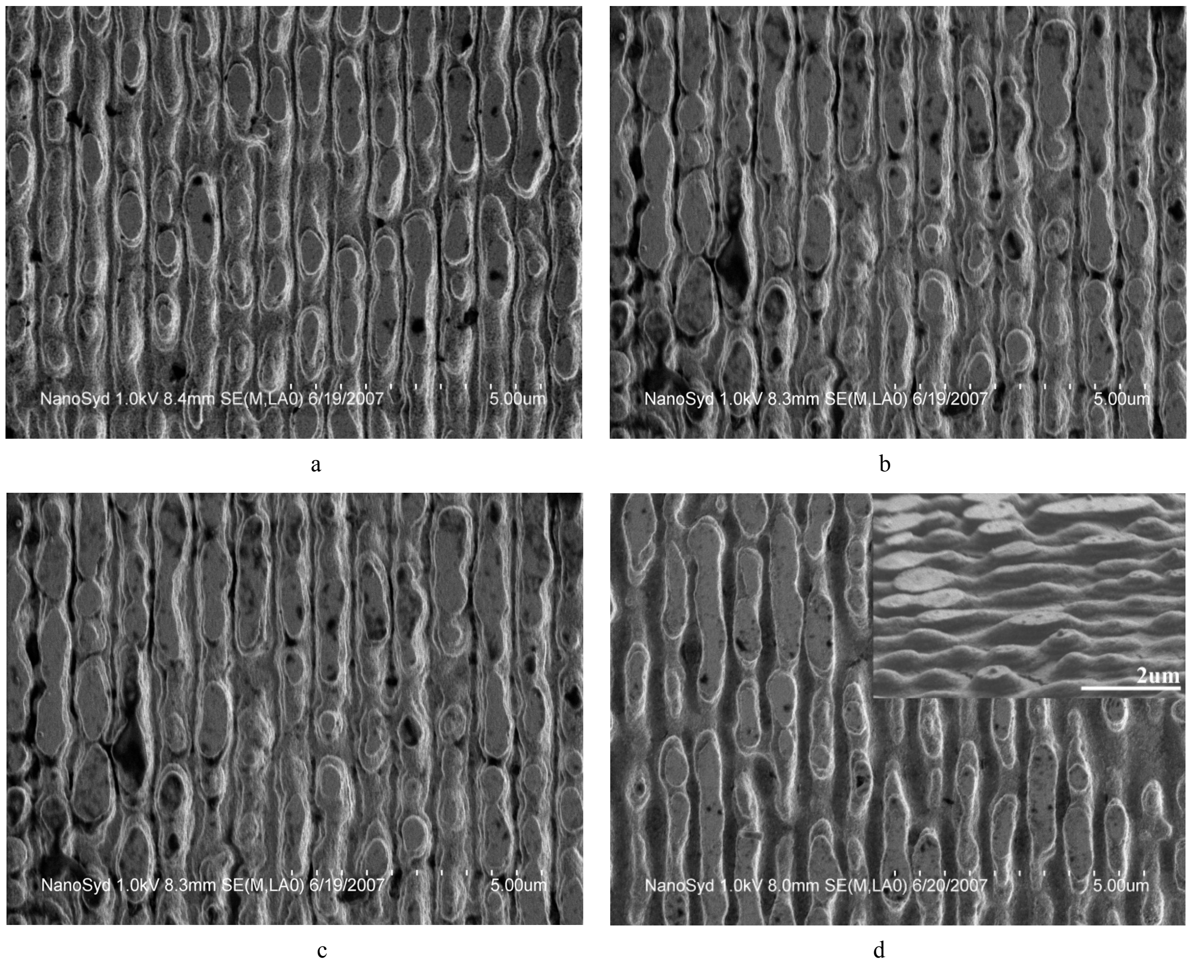

Fig. 3. SEM micrographs of the nickel shim with different "3" "A" and "3" "B" sublayers: a – sample "A", "R" area, b – sample "A", "H", c – sample "B", "R", d – sample "B", "H" (the inset in d shows 3D view of the nickel shim tilted under 25°)

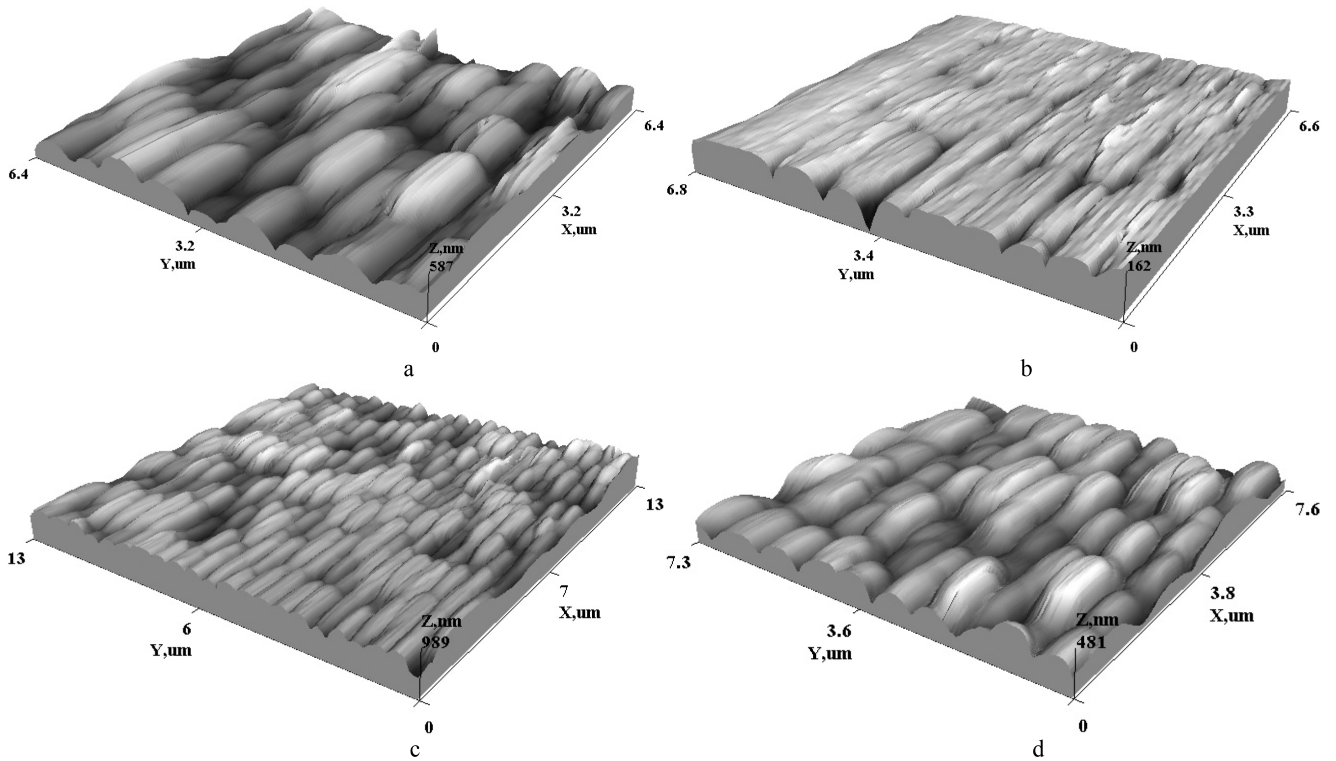

Fig. 4. AFM images of the nickel shim with different "3" "A" and "3" "B" sublayers: a – sample "A", "R" area, b – sample "A", "H", c – sample "B", "R", d – sample "B", "H"

4. CONCLUSIONS

1. We have assembled and optimized custom design laser beam interference lithography optical scheme using diffraction grating as a beam splitter for recording interference pattern of two laser beams through set of masks in a photoresist (high diffraction efficiency diffraction gratings). Our optical setup enables producing of submicron period diffraction gratings (at least 8 set of masks and 9 orientation and different submicrometer range) changing the angle between the interfering beams.

2. Evaluation of the geometrical parameters of microrelief structures in each step of manufacturing was performed using "PCGrate" software (based on the modified integral method) and diffraction efficiency measurements. Results obtained using different computer simulated and experimental methods show good correlation. The results show that during the transfer process both depth and period of the sinusoidal profile gratings originally produced in a photoresist is decreased.

3. Both investigated sublayers (Cu and Ni) coated by vacuum deposition are shown to be efficient and geometrical parameters of the grating are transferred efficiently and independently of the used sublayer.

Acknowledgments

This work was financially supported by Lithuanian Science and Studies Foundation and NordForsk. Authors acknowledge head of NanoSYD group prof. Horst-Günter Rubahn for the SEM facilities.

REFERENCES

1. **Leech, P. W., Lee, R. A.** Optically Variable Micro-mirror Arrays Fabricated by Graytone Lithography *Microelectronic Engineering* 83 2006: pp. 351 – 356.
2. **Leech, P. W., Sexton, B. A., Marnock, R. J.** Scanning Probe Microscope Analysis of Microstructures in Optically Variable Devices *Microelectronic Engineering* 60 2002: pp. 339 – 346.
3. **Grigaliūnas, V., Jucius, D., Tamulevičius, S., Guobienė, A., Kopustinskas, V.** Optically Variable Imaging Using Nanoimprint Technique *Applied Surface Science* 245 2005: pp. 234 – 239.
4. **Leech. P. W., Sexton, B. A., Marnock, R. J., Smith, F.** Fabrication of hologram coins using electron beam lithography *Microelectronic Engineering* 71 2004: pp. 171 – 176.
5. **Leech, P. W., Lee, R. A.** Hot Embossing of Diffractive Optically Variable Images Inbiaxially-oriented Polypropylene *Microelectronic Engineering* 83 2006: pp. 351 – 356.
6. **Xie, Q., Hong, M. H., Tan, H. L., Chen, G. X., Shi, L. P., Chong, T. C.** Fabrication of Nanostructures with Laser Interference Lithography *Journal of Alloys and Compounds* 2007 (Article in press).
7. **Tamulevicius, T., Tamulevicius, S., Andrulevicius, M., Griskonis, E., Puodziukynas, L., Janusas, G., Guobiene, A.** Formation of Periodical Micro Structures Using Interference Lithography *Experimental Techniques* 2006 (Article in press).
8. **Tamulevičius, S., Guobienė, A., Janušas, G., Palevičius, A., Ostaševičius, V, Andrulevičius, M.** Optical Characterization of Diffractive Optical Elements Replicated in Polymers *Journal of Microlithography Microfabrication and Microsystems* 5 (1) Art. No. 013004, Jan-Mar 2006: pp. 807 – 814.
9. **Palmer, Ch., Loewen, E.** Editor (First Edition) /Diffraction Grating Handbook 4th Edition USA 2000: 145 p.
10. The "PCGrate" Software is Available from International Intellectual Group, Inc. (I.I.G., Inc.) www.iigrate.com.
11. **Seely, J. F., Goray, L. I., Kjornrattanawanich, B., Laming, J. M., Holland, G. E., Flanagan, K. A., Heilmann, R. K., Chang, C.-H., Schattenburg, M. L., Rasmussen, A. P.** Efficiency of a Grazing-incidence Off-plane Grating in the Soft–X-ray Region *Applied Optics* 45 (8) 2006: pp. 1680 – 1687.
12. **Tamulevičius, T., Tamulevičius, S., Andrulevičius, M., Janušas, G., Guobienė, A.** Optical Evaluation of Geometrical Parameters of Micro-Relief Structures *Materials Science* (*Medžiagotyra*) 12 (4) 2006: pp. 360 – 365.
13. **Tamulevičius, T., Tamulevičius, S., Andrulevičius, M., Janušas, G., Ostaševicius, V., Palevičius, A.** Optical Characterization of Microstructures of High Aspect Ratio *Proceedings of SPIE,* Vol. 6518, *Metrology, Inspection, and Process Control for Microlithography* XXI, Chas N. Archie, Editor, 65183Q (Apr. 5, 2007).